Maternal microbiota *Bifidobacterium* promotes placental morphogenesis, nutrient transport and fetal growth in mice

Authors: Jorge Lopez-Tello[1]*, Zoe Schofield[2]*, Raymond Kiu[2], Matthew J. Dalby[2], Douwe van Sinderen[3], Gwénaëlle Le Gall[4], Amanda N Sferruzzi-Perri[1†], Lindsay J Hall[2,5†]

Affiliations:

[1]Department of Physiology, Development, and Neuroscience, Centre for Trophoblast Research, University of Cambridge, Cambridge, UK

[2]Gut Microbes & Health, Quadram Institute Bioscience, Norwich Research Park, Norwich, UK

[3]APC Microbiome Institute, University College Cork, Cork, Ireland

[4]Norwich Medical School, University of East Anglia, Bob Champion Research and Education Building, James Watson Road, Norwich Research Park, Norwich NR4 7UQ, UK

[5]Chair of Intestinal Microbiome, School of Life Sciences, ZIEL – Institute for Food & Health, Technical University of Munich, Freising, Germany

[*†]Contributed equally

Corresponding author names:

Jorge Lopez-Tello (jl898@cam.ac.uk)

Amanda N. Sferruzzi-Perrri (ans48@cam.ac.uk)

Lindsay J Hall (Lindsay.Hall@tum.de **I** Lindsay.Hall@quadram.ac.uk)

Author Contributions: JL-T, ZS, ANS-P, LJH designed research; JL-T, ZS, RK, GLG conducted research, JL-T, ZS, RK, MJD contributed analytic tools and performed analysis; DvS contributed reagents; JL-T, ZS, ANS-P, LJH wrote the paper with feedback from all the authors.

Competing Interest Statement: The authors declare that they have no competing interests.

Classification: Biological Sciences, Microbiology, Physiology, Metabolism, Development

Keywords: Pregnancy, Placenta, Microbiota, Fetus, *Bifidobacterium*

Abstract

The gut microbiota plays a central role in regulating host metabolism. However, while substantial progress has been made in discerning how the microbiota influences host functions post birth and beyond, little is known about how key members of the maternal gut microbiota can influence feto-placental growth. Here, using germ-free and specific-pathogen-free mice, we demonstrate that the bacterium *Bifidobacterium breve* UCC2003 modulates maternal body adaptations, placental structure and nutrient transporter capacity, with implications for fetal metabolism and growth. The effects of *B. breve* UCC2003 on feto-placental growth are mediated, in part, by changes in the maternal and placental metabolome (*i.e.* acetate and carnitine). Histological analysis of the placenta confirmed that *Bifidobacterium* modifies placental structure via changes in *Igf2P0, Dlk1, Mapk1* and *Mapk14* expression. Additionally, *B. breve* UCC2003*,* acting through *Slc2a1* and *Fatp1-4* transporters, was shown to restore fetal glycaemia and fetal growth in association with changes in the fetal hepatic transcriptome. This study provides knowledge towards a novel and safe therapeutic strategy for treating pregnancy disorders via modulation of the maternal gut microbiota.

Introduction

All nutrients and metabolites required for feto-placental growth are provided by the mother, which in turn is thought to be influenced by the maternal gut microbiota through breakdown of complex dietary components [1]. During gestation, liberated metabolites may be used by the placenta for morphogenesis, and transported across the placenta for use by the fetus for growth and development [2,3]. This is highly important across gestation, particularly at later stages, when fetal growth is maximal. Notably, there are also alterations in the maternal

microbiota throughout pregnancy with levels of the beneficial bacterial genus *Bifidobacterium* rising from trimester 1 onwards [4–6]. Failure of the mother to provide nutrients and metabolites to the fetus can result in pregnancy complications including small for gestational age (SGA), fetal loss and stillbirth. However, the contribution of the maternal microbiota in determining fetal outcomes is largely unexplored. Knowledge in this area would be highly valuable for developing treatments to improve fetal growth, with benefits for population health.

Studies performed with Germ free (GF) mice have identified that the microbiota is a key regulator for adequate development, early immune education and metabolism [7–11]. However, little is known about how maternal microbiota influences feto-placental growth and more specifically, placental structure and function. Here, we hypothesized that the maternal gut microbiota, and specific microbiota members, regulate fetal growth by modulating placental development and nutrient supply. We tested this hypothesis by comparing conceptus growth across a range of microbiome complexity; using conventional specific-pathogen-free (SPF) mice as a model for standard microbial colonization, and as a base line to define correct feto-placental growth [11], GF mice which represent a completely clean and naïve microbiome system, and finally a mono-colonized maternal GF model – GF mice colonized with *Bifidobacterium breve* UCC2003 [12]. As a keystone microbiota member and 'probiotic' species, *B. breve* may represent a suitable option for treating pregnancy complications by exerting beneficial metabolic effects on maternal physiology and associated feto-placental growth. Indeed, *B. breve* induced changes in maternal physiology, placental morphogenesis and the abundance of placental glucose and lipid transporters, which were associated with improvements in growth and metabolism of the fetus.

Results

Germ-free mice treated with B. breve have altered body composition and caecum metabolic profile

To assess whether maternal microbiota is able to influence feto-placental growth, GF mice were treated orally with *B. breve* UCC2003 from day 10 of gestation (treatment on days 10, 12 and 14; i.e. BIF group), and compared to GF and SPF dams (for experimental overview see Figure 1A). Timing and dosing were based on the fact that levels of *Bifidobacterium* rise throughout pregnancy (5) (colonization levels during pregnancy can be found in Figure S1). Moreover, previous work has indicated three consecutive doses of *B. breve* UCC2003 facilitates stable gut colonization, with the advantage of also avoiding repeated handling of the mice, which may induce spontaneous abortions [13,14]. In addition, from a translational point of view, we also wanted to correlate our animal model with potential future supplementation studies in women at the point pregnancy is confirmed.

Maternal body composition differed between groups with GF and BIF mice showing increased digestive tract weight and lower pancreas mass compared to SPF mice. GF and BIF mice had similar circulating concentrations of glucose and insulin to SPF mice (assessed in fed conditions; Table 1). Compared to SPF mice, treatment with *B. breve* reduced maternal gonadal fat depot, liver, and spleen weights in BIF mice. No differences were observed in the circulating concentrations of leptin, cholesterol, triglycerides, or free fatty acids in maternal serum (Table 1).

Metabolomics analysis in maternal caecum samples indicated that the concentration of 13 out of 81 metabolites were significantly altered (Table 1 and Table S1). Acetate was influenced by *B. breve* (Table 1), with BIF dams having intermediate concentrations compared to SPF and GF mice (the low levels of acetate detectable in GF mice, most likely originated from the diet and/or are host-derived). These findings suggest that acetate producing *B. breve* and the wider gut microbiota may exert selective effects on maternal metabolic (gonadal fat depot and liver) and immune organs (spleen).

Maternal gut microbiota and B. breve regulate fetal growth by controlling fetal glycaemia

Although the three experimental groups had similar numbers of viable fetuses per litter, the GF group had higher numbers of resorptions within the litter (defined as small hemorrhagic-to-black implantation sites, without presence of fetal development) compared to SPF and BIF mice (Figure 1B-C). Similarly, when this parameter was calculated as resorption rate (number of resorptions divided by total litter size) we found similar results (Figure S2). In fact, all GF dams had at least one resorption, whilst *B. breve* reduced the appearance of resorptions by 50% (Figure 1C and Figure S2). No evidence of intrauterine death, defined as a lack of fetal vascular flow in the yolk sac vessels, or macerated fetus were found (classification of resorption or fetal death was based on previous work[15]). Compared to SPF and BIF mice, GF fetuses were growth restricted, hypoglycaemic and had reduced liver weight, but had preserved brain size (Figure 1D-F). These findings highlight that the maternal microbiota influence fetus viability and that *B. breve* is a strong modulator of fetal growth and metabolism.

Maternal B. breve modulates fetal hepatic transcriptome

The liver is a key organ for glucose storage and production. As fetuses from BIF mice had enlarged livers and improved glycaemia, we next determined if there were changes in the fetal hepatic transcriptome (livers were collected on GD18.5, when fetal liver function is particularly active prior to term. Indeed, mouse fetal hepatocytes are mature from GD18.5, when they present a similar gene expression pattern to those in the postnatal liver [16]). A total of 602 genes were differentially expressed, with 94 significantly up-regulated and 508 down-regulated genes in BIF group, when compared to GF group (Figure 1G-H). Functional enrichment analysis indicated many metabolic pathways were regulated in the fetal livers of BIF mice including carboxylic acid and lipid metabolic processes, steroid hydroxylase activity, fatty acid metabolism and response to glucocorticoid (Figure 1I-J; Table S2). Therefore, maternal *B. breve* appears to exert beneficial alterations in fetal hepatic function to support fetal growth.

Maternal gut microbiota and B. breve control placental morphogenesis

To further understand the links between the maternal microbiota and the regulation of fetal growth, we assessed placental structure (performed on GD16.5, when placental growth in mice is maximal [17]. Only viable fetuses were analysed). When compared to SPF mice, placentas were lighter in GF and BIF mice (Figure 2A). Placental efficiency, defined as the grams of fetus produced per gram of placenta, was significantly improved in the BIF group compared to GF mice (Figure 2B). Analysis of placental compartments showed that lack of maternal gut microbiota significantly hampered growth of the placental labyrinth transport zone (Lz), without compromising the endocrine junctional zone or decidua volumes (Figure 2C). It also did not affect placental glycogen storage (Figure 2D) or the volume of the trophoblast

(Figure E-F). Analysis of maternal blood spaces revealed that GF and BIF groups had reduced spaces compared to SPF mice, while the volume and the length of fetal capillaries were significantly reduced in the GF compared to SPF (Figure 2F-G). Similarly, surface area for exchange of the Lz was significantly decreased in GF compared to SPF mice (Figure 2H). The barrier between maternal and fetal blood was also determined to be thinner in BIF *versus* GF mice (Figure 2I). Lz apoptosis levels were similar between groups (Figure 2J).

To define the molecular mechanisms behind the changes in the Lz, we quantified the expression of select genes in micro-dissected Lz. The angiogenic factor *Vegf* was similarly expressed between groups (Figure 2K). However, the expression of signaling pathways involved in cell proliferation and growth, namely the MAPK pathway, was significantly altered by changes in maternal gut microbiota; *Mapk1* was shown to be increased in both GF and BIF, while *Mapk14* (also known as *p38Mapk*) was revealed to be specifically up-regulated in the Lz of BIF mice. In addition, *Dlk1* and *Igf2P0*, which are key genes implicated in metabolism and Lz formation, were significantly up-regulated in the BIF group compared to GF mice. The expression of *Akt* did not vary with group (Figure 2K). As informed by western blotting, activation of ERK was reduced in the placental Lz of GF compared to SPF mice, and this effect was reversed by BIF (Figure 2L). p38MAPK protein activity was similar between groups. DLK1 protein level was also lower in GF compared to SPF mice. However BIF increased DLK1 protein levels when compared to both SPF and GF mice (Figure 2L). Overall, these findings suggest that the maternal gut microbiota, and *B. breve*, regulate the development of the mouse placental Lz via modulation of specific cell growth and metabolic genes/pathways.

Maternal gut microbiota and B. breve controls key placental nutrient transporters

Glucocorticoids are a class of steroid hormones that can affect both fetal and placental formation. To control glucocorticoid actions on the conceptus, the placenta expresses 11β-hydroxysteroid dehydrogenase type 1 and 2 (*11Hsd1* and *11Hsd2*). We found that the expression of *11Hsd1* trended to be elevated in the BIF group compared to the GF (P=0.09; no change in *11Hsd2*; Figure 2M). Moreover, to better understand the changes in fetal growth and glycemia between groups, we quantified the expression of selected amino acid, glucose and lipid transporters in the Lz. We found no difference in the expression of system A amino acid transporters (*Slc38a1, Slc38a2, Slc38a4*) between groups (Figure 2N). However, the key glucose transporter *Slc2a1* was up-regulated in the Lz of BIF mice compared to GF mice (*Slc2a3* mRNA levels were similar between groups; Figure 2O). Fatty acid transporters were also altered, with increased levels of *Fatp1* in the GF group compared to SPF and BIF, while *Fatp4* was increased in the BIF group compared to the GF (Figure 2P; *Cd36* and *Fatp3,6* expression levels were unaltered). Collectively, these data suggest that maternal gut microbiota, and *B. breve*, regulate fetal growth by inducing changes in the expression of key nutrient transporters within the placenta.

Differences in placental labyrinth growth are linked to an altered placental metabolome

To gain further mechanistic understanding of the changes observed in the placental Lz and fetal liver, we analysed >80 metabolites at GD16.5 (Figure 3 and Table S1). We found 5 metabolites significantly altered in the placental Lz (Figure 3). 2-Aminoadipate in the Lz was very low in GF/BIF groups as well as in fetal livers (Figure 3A). Treatment with *B. breve* significantly reduced the concentrations of acetylcarnitine and carnitine in Lz tissue compared

to SPF placentas, but not in fetal livers (Figure 3B-C). Levels of formate in placental Lz were significantly elevated in both GF and BIF compared to SPF mice (Figure 3D), with a similar trend (although not significant) in fetal liver samples. Acetate was also altered in the Lz (Figure 3E), with concentrations significantly lower in the SPF compared to the GF group, whilst BIF samples showed intermediate levels (although these levels were much lower than observed in the maternal caecum). Similar to formate, concentrations of acetate in fetal liver followed similar directions to the Lz, yet were not statistically different between groups. These data suggest that maternal gut microbiota, and *B. breve*, regulate the fetal and placental growth via modulation of the placental Lz metabolome.

Discussion

In this study, we provide evidence that the maternal microbiota and the microbiota member *B. breve* regulate maternal body composition during gestation and beneficially modulate feto-placental growth. To the best of our knowledge, this is the first demonstration of a maternal gut bacterium remotely controlling placental structure and nutrient transporters, with important implications for fetal glycaemia and fetal growth. We observed that the effects of *Bifidobacterium* are partially mediated by altered metabolites in maternal caecum and in placental Lz tissue, with alterations in the expression of key genes in the placental Lz and fetal liver.

Bifidobacterium is the dominant microbiota member in vaginally delivered, breast fed infants, with certain species and strains known to stimulate and aid the maturation of the immune system [18]. *B. breve* UCC2003 also regulates responses at the gut barrier, inducing

homeostatic epithelial cell programming, and protecting against inflammatory insults [14,19]. Importantly, pregnancy is accompanied by increasing *Bifidobacterium* abundance in the gut of women and mice [5], which is associated with changes in progesterone concentrations during pregnancy. Additionally, alterations in the abundance of *Bifidobacterium* are also linked to the development of serious pregnancy complications like preeclampsia [20]. Our study shows that *B. breve* improves pregnancy outcomes in mice, as indicated by elevated placental efficiency and restored fetal glycaemia and weight. *B. breve* UCC2003 was also shown to induce changes in the metabolite milieu, including acetate, acetylcarnitine and carnitine in the mother and placenta, which were likely key for the beneficial effects on fetal growth. Acetate is a major bifidobacterial fermentation by-product, which directly mediates epithelial cell responses but also exerts systemic beneficial metabolic effects [21,22]. More generally, microbial-derived short-chain fatty acids (SCFAs) modulate multiple host physiological systems and during pregnancy are associated with maternal gestational weight, neonatal length and body weight, and protection against allergic airway disease in the developing fetus [23,24]. Acetate crosses the placenta [24], so in our model, the elevated maternal *B. breve*-derived acetate may exert beneficial effects on feto-placental growth via (i) maternal effects, through interactions within the maternal gut mucosa as evidenced by higher maternal caecum acetate concentrations in *B. breve* supplemented (and SPF dams vs. GF) and the subsequent impact on maternal organs (liver, adipose and spleen) and nutrient handling, (ii) effects on the placenta, through use of acetate for cellular metabolism, growth and function, and/or (iii) effects on the fetal metabolism following transport of acetate across the placenta to the fetus. Compared to the maternal caecum, levels of acetate were relatively low in the placental Lz and fetal liver (for all 3 groups). This suggests that *B. breve* (and SPF microbiota-derived acetate) may be used to

support anabolic processes *in utero* (hence the very low levels detected), and together with changes in acetylcarnitine and carnitine, may be supported by our observations of elevated fatty acid transporter expression in the placenta and differentially regulated genes in the fetal liver. The observed modulation of immune-associated pathways in the fetal liver, including those associated with G protein-coupled receptor signalling (e.g. *Dusp9*), also indicates a role for direct acetate-associated responses [25]. *B. breve* supplementation also restored fetal glycaemia and weight in BIF mice, achieving similar values to that seen for SPF fetuses. Previous *in vivo* studies indicate different strains of *Bifidobacterium* (including *B. breve*) modulate glucose handling [26], with this genus also consistently associated with potential protection against human metabolic disorders e.g. type 2 diabetes [27,28]. In addition, our observations of reduced maternal gonadal fat mass and maternal liver weight in *B. breve*-treated dams compared to SPF dams, suggest that *Bifidobacterium,* or *B. breve* metabolites, could affect maternal metabolic responses in key organs of the mother. In fact, previous work in adult mice suggests elevation of gut acetate levels due to *Bifidobacterium* treatment plays a key role in regulating glucose handling systemically and reduces visceral fat accumulation [29].

Maternal microbiota significantly affected the placental vascular bed, which is required for adequate fetal growth [30]. Moreover, *B. breve* significantly reduced the interhaemal membrane barrier thickness of the placenta, which may facilitate exchange of nutrients and gases. The mechanisms governing these structural changes could be partially mediated by changes in the expression of two imprinted genes [31], *Igf2* (namely the placenta-exclusive isoform, *Igf2P0*) and *Dlk1*, and via MAPK upregulation. In this regard, deletion of *Igf2P0* results in feto-placental growth restriction in association with reduced placental surface area for exchange, fetal

capillary volume and increased barrier thickness (reviewed by [32]); parameters that were partially improved by *B breve* UCC2003 in line with the *Igf2P0* mRNA upregulation. Interestingly, *Igf2P0* is important for the structural and transport adaptations occurring in the placenta in response to maternal nutritional restriction [33] and recent work has shown that *Igf2* in the placenta interacts with MAPK signaling [34]. *Dlk1,* a non-canonical ligand of the Notch signalling pathway localized to the endothelial cells of fetal capillaries in the placental Lz, also regulates placental vascularisation and branching morphogenesis [35]. In addition, IGF2 and DLK1 can both mediate cellular actions via the MAPK pathway [36,37]. *Mapk14*, also known as p38MAPK, forms part of a signal transduction pathway that has been linked to environmental stresses and inflammatory cytokines [38]. However, p38MAPK also regulates many normal cellular processes, including proliferation and cytoskeletal organisation. Furthermore, research in mice has demonstrated that *Mapk14* is essential for embryogenesis and placental Lz angiogenesis and vascular remodeling [39]. In addition, placentas exposed to *B. breve* UCC2003, had lower concentrations of acetylcarnitine and carnitine compared to SPF, suggesting a greater reliance on these compounds for energy production, or enhanced transfer of these fatty acids to the fetus [40]. Carnitine is well-known for mediating the transport of fatty acids into mitochondrial matrix for fatty acid β-oxidation. Carnitine can also promote p38MAPK signalling activation in cardiac tissue [41]. Taken together, placental structural, transport and metabolic changes seen with *B. breve* UCC2003 treatment may link to the altered metabolites/nutrient milieu in the mother and would have been beneficial in providing additional substrates for fetal growth and development (when compared to GF).

While our study has clear strengths and strong translational implications for pregnancy complication treatments, it also has certain limitations. Unsurprisingly, we did not see a full 'rescue' of placental phenotype in the monocolonised GF *B. breve* (BIF) group, compared to complex microbiota found in SPF dams. However, structural and functional adaptations of these placentas exposed to *B. breve* were adequate enough to 'rescue' fetal weight and fetal glycaemia. An array of gut-associated signaling and a diverse metabolite pool are expected to provide more complete placental development. Indeed, other or additional *Bifidobacterium* species and/or strains may be required for placental and fetal development, given strain-specific host physiology responses [19,42]. Further studies should allow the relative contributions of other microbial- and *Bifidobacterium*-derived factors to be elucidated. In addition, future work should evaluate the response of pregnant SPF mice to *B. breve* UCC2003 and the contribution of *B. breve* in mediating changes in embryo/fetal viability (litter resorption rate). Previous work undertaken in GF *versus* SPF mice [11] showed that GF mice have increased resorptions compared to SPF mice, suggesting a potential crosstalk between the female gut and genital tract microbiota [43]. Here, we reported that *B. breve* supplementation increased embryo/fetal viability in GF mice. However, to verify this effect, future work should analyze embryo/fetal viability each day of the supplementation period and use larger cohorts of SPF and GF pregnant mice. It would also be valuable to assess the impact of *B. breve* supplementation from prior to, and/or during the whole pregnancy. Nonetheless, this study has revealed novel roles for *Bifidobacterium* and provides a safe therapeutic strategy for treating pregnancy complications, suggesting an opportunity for *in utero* programming through maternal *Bifidobacterium* and associated metabolites.

Overall, although our study was performed in mice and is not representative of a clinical scenario, our study highlights the importance of the maternal gut microbiota during gestation and demonstrates that *B. breve* modulates maternal physiology, placental structure and nutrient transporter capacity with impact on fetal glycaemia and fetal growth (Figure 4). Our findings prompt an in-depth investigation into how additional members of the gut microbiota impact on pregnancy outcomes. These future studies are important for the design of novel therapies to combat fetal growth restriction and other pregnancy complications.

Materials and Methods

***Bifidobacterium breve* UCC2003/pCheMC**

B. breve UCC2003/pCheMC was generated by introducing the plasmid pCheMC to electrocompetent *B. breve* UCC2003 as described previously [44]. In brief, *B. breve* UCC2003 was grown until mid-log phase, chilled on ice and washed twice with ice cold sucrose citrate buffer (1mM citrate, 0.5M sucrose, pH5.8) and then electroporation of cells was carried out under the following conditions; 25 MF, 200 Ohms, 2 KV. Transformed cells were incubated for 2 hours in Reinforced Clostridial Medium (RCM) at 37□C in a controlled anaerobic chamber then plated [45] on RCM agar plates with selective antibiotics. Colonies were sub-cultured 3 times on RCM agar plates with selective antibiotics. Antibiotics were used at the following final concentrations erythromycin 2µg/mL.

Lyophilised *B breve*

B. breve was grown in De Man, Rogosa and Sharpe agar (MRS) under anaerobic conditions overnight. The bacterial cell pellet was resuspended in 10% milk powder and lyophilised in

200ml quantities. Lyophilised *B. breve* was reconstituted with 500µl PBS. Concentration of *B. breve* was 10^{10}CFU/ml. All batches were tested for contamination upon reconstitution on Luria-Bertani (LB) and Brain-Heart Infusion (BHI) plates under anaerobic and aerobic conditions at 37°C. No contamination of *B. breve* was detected.

Mice

All mouse experiments were performed under the UK Regulation of Animals (Scientific Procedures) Act of 1986. The project license PDADA1B0C under which these studies were carried out was approved by the UK Home Office and the UEA Ethical Review Committee. All mice were housed in the Disease Modelling Unit at the University of East Anglia, UK. Animals were housed in a 12:12 hour light/dark, temperature-controlled room and allowed food and water *ad libitum* (food/water intake was not recorded). Female Germ Free C57BL/6J (GF) and Specific Pathogen Free (SPF) mice aged 6-8 weeks were used for the study. GF mice were bred in germ free isolators (2 females to 1 male) and on gestational day (GD) GD9.5, pregnant mice (confirmed by weight gain) were removed from the GF isolator and transferred to individually ventilated cages. The sterility of these cages was previously tested and found to be suitable for housing GF mice for 1 week. Sterile water was changed every 2 days. We assessed responses at 2 gestational phases – the majority of studies were carried out at GD16.5, whilst the RNASeq studies utilized fetal livers harvested at GD18.5. A total of 6 SPF mice were used for GD16.5 assessments (no SPF mice were studied on GD18.5). For the GF a total of 5 (GD16.5) and 3 (GD18.5) dams were used. For the BIF mice, a total of 6 (GD16.5) and 4 (GD18.5) dams were used.

***B. breve* colonisation levels**

Mice were given 100µL of reconstituted lyophilised *B. breve* UCC2003 by oral gavage (containing 10^{10} CFU/mL) at GD10, GD12 and GD14 or 100µL vehicle control (PBS, 4 % skimmed milk powder), with this dosing regimen reflecting a more realistic time frame for women who are more likely to start taking probiotics once their pregnancy is confirmed. At GD16.5 and GD18.5, mice were sacrificed by cervical dislocation and samples collected for molecular and histological analysis. The experimental design can be found in Figure 1A.

Faecal samples were checked for contamination and *B. breve* colonization at GD12 and GD14 and GD16. Briefly, faecal samples from GF and BIF mice were diluted in 500 µL of PBS and agitated for 30 mins at 4˚C on an Eppendorf MixMate 5353 Digital Mixer Plate Shaker. The faecal solution was passed through a 0.45µm syringe filter. Faecal solution was diluted 1 in 100 and 20 µL was added to a De Man, Rogosa and Sharpe agar plate with erythromycin and incubated for 48 hours in an anaerobic chamber at 37˚C. Colony forming units were counted using a click counter.

Blood hormones and circulating metabolites

Maternal blood was obtained by cardiac exsanguination immediately after cervical dislocation. Blood was centrifuged and serum collected and stored at -80ºC until further analysis. Blood glucose and plasma concentrations of leptin, insulin, triglycerides, cholesterol, and free fatty acids were determined as previously reported [46]. Fetal blood glucose levels were measured with a handheld glucometer (One Touch Ultra; LifeScan) immediately after decapitation of the fetus (fetuses were selected at random).

Placental histology

Placentas were cut in half and fixed in 4% paraformaldehyde overnight at 4ºC. Samples were washed 3 times with PBS for 15 minutes each and storage in 70% ethanol until embedding in wax. Embedded placentas were cut at 5µm thickness and stained with haematoxylin and eosin for gross morphology. Placental layer volumes were calculated using the Computer Assisted Stereological Toolbox (CAST v2.0). For analysis of labyrinth components, sections were stained with lectin for identification of fetal endothelial vessels and with cytokeratin for trophoblasts. Further details of the double-labelling immunohistochemistry and the analysis performed can be found elsewhere [47]. For the analysis of placental glycogen, sections were stained with Periodic acid–Schiff (Sigma-Aldrich) previous incubation with 0.5% periodic acid (Thermo Fisher Scientific). Sections were counterstained with Fast-green (Sigma-Aldrich) and digitalized with the nanozoomer scanner (Hamamatsu). Analysis of placental glycogen accumulation was performed with Image J and conducted blinded to experimental groups. TUNEL staining for placental cell death was performed using the TUNEL Assay Kit - HRP-DAB (Abcam, ab206386) following manufacturer instructions except for the counterstaining which was substituted for Nuclear Fast Red (Vector). Sections were digitalized using a nanozoomer scanner (Hamamatsu) and the amount of apoptosis in the labyrinth zone was calculated in 5 random areas (x20 magnification) and analysed by Image J software.

Western blotting

Protein extraction was performed with RIPA buffer as described previously [48]. Lysates were separated by SDS-PAGE and incubated with antibodies against p-MAPK (Thr202/Tyr204)

(Cell Signalling, 4370; 1/1000), t-MAPK 44/42 (Cell Signalling, 4695; 1/1000), DLK-1 antibody (Abcam, ab21682; 1/1000), p-P38MAPK (Cell Signalling, 4511; 1/1000) and t-P38MAPK (Cell Signalling, 8690; 1/1000). Reactive bands were detected by chemiluminescence (Thermo Scientific, Scientific SuperSignal West Femto) and quantified by Image J software. Proteins were normalized to Ponceau S Staining [49].

RNA extraction and qPCR

Extraction of RNA from micro-dissected placental labyrinth zones was performed with RNeasy Plus Mini Kit (Qiagen) and reverse transcribed using the High Capacity cDNA RT Kit minus RT inhibitor (Applied Biosystems) according to manufacturer's instructions. Samples were analysed using MESA Blue SYBR (Eurogentec) and primers (See Supplementary Table 3) were synthesized by Sigma-Aldrich. The expression of each gene was normalized to the geometric mean expression of two reference genes *Hprt* and *Ubc*, which remained stably expressed across the groups. Analysis was performed using the 2-ΔΔCt method [50].

Sequence pre-processing, Differential Gene Expression (DGE) analysis and Functional enrichment analysis

Fetal liver RNA on GD18.5 was extracted using the RNeasy Plus Mini Kit (Qiagen). RNA sequence pre-processing and DGE analysis was performed as previously described with slight modifications [14]. Briefly, FASTQ reads were initially quality-filtered using fastp v0.20.0 with options -q 10 (sequence reads with phred quality <10 were discarded). Subsequently, sequence reads for each sample were merged (merge-paired-reads.sh) and followed by rRNA sequence filtering via SortMeRNA v2.1 based on SILVA rRNA database optimised for

SortMeRNA software [51,52]. Filtered reads were then unmerged (unmerge-paired-reads.sh) and ready for transcript quantification. Transcript mapping and quantification were then performed using Kallisto v0.44.0 [53]. *Mus musculus* (C57BL/6 mouse) cDNA sequences (GRCm38.release-98_k31) retrieved from Ensembl database were indexed with Kallisto utility *index* at default parameter and was used for following transcript mapping and abundance quantification via Kallisto utility *quant* at 100 bootstrap replicates (-b 100) [54].

RNA raw counts were subjected (Kallisto outputs) to DGE analysis, which was performed using R library *Sleuth* (v0.30.0) [55]. Transcripts were then mapped to individual genes using Ensembl BioMart database (GRCm38.p6) with function *sleuth_prep* and option *gene_mode* = *TRUE*. Genes with an absolute $\log_2$ (fold change) >1.0 and q value <0.05 (p-adjusted value; based on Wald test statistics) were considered to be differentially regulated [56]. DGE statistics were plotted via functions within package *Sleuth*. Finally, functional enrichment analysis was performed using g:Profiler webtool g:GOst based on organism *Mus Musculus* species [57]. Briefly, a list of DGEs (Ensembl IDs) was uploaded to g:GOst, then selected 'GO molecular function', 'GO biological process' and 'Reactome' in the 'data sources'. Significance threshold was set at 0.001 (g:SCS threshold).

Metabolite extraction, Nuclear Magnetic Resonance (NMR) spectroscopy and metabolite quantification

Extraction of metabolite from liver, placenta, caecum contents and culture (spent) media samples were performed as previously described as a standard protocol [58]. For caecal samples, frozen materials (stored at -80°C prior to analysis) were weighed ~50 mg before the

addition of 600 µL of faecal water phosphate buffer solution. The faecal water phosphate buffer was prepared as follows: add 0.51g $NaH_2PO_4.H_2O$ and 2.82g K_2HPO_4 to 200 mL D_2O (Deuterium Oxide; Merck). To this, 34.5 mg TSP (Trimethylsilyl propanoic acid; used as NMR standard) and 100 mg NaN_3 (Merck) were added [59]. Next, the mixture was centrifuged for 10 min at 17,000 x g before transferring the mixture to an NMR tube (Merck) for subsequent NMR analysis.

For liver and placenta samples (stored at -80°C prior to analysis), frozen fresh tissue (~20-45 mg) was placed into a 2 ml sterile microcentrifuge tube pre-loaded with ~15-20 glass beads (Merck) while 200 µL of ice-cold methanol (Fisher Scientific) and 42.5 µL of ultra-pure cold water were added to it and vortexed. Tissue was disrupted via a tissue lyser (Qiagen) for 2 x 2 mins. 100 µL of ice-cold chloroform (Merck) was then added and vortexed. 100 µL of ice-cold chloroform and 100 µL of ultra-pure cold water were added to the mixture, and kept on ice for 15 min. Liquid was then transferred into a new sterile microcentrifuge tube and centrifuged for 3 min at 17,000 x g. The top aqueous phase was transferred into a new microcentrifuge tube and speed-vacuumed for 30 min at 50°C and 30 min without heating prior to reconstitution with faecal water phosphate buffer solution at 600 µL. The mixture was then moved to an NMR tube (Merck) for subsequent NMR analysis. Metabolites from culture media Brain Heart Infusion (BHI; Oxoid) and spent media (BHI cultured with *B. breve* UCC2003 for 48 h) were extracted as follows: 400 µL of medium was transferred into a sterile microcentrifuge tube with the addition of 200 µL faecal phosphate buffer and mixed well. The mixture was then moved to an NMR tube (Merck) for further NMR analysis.

Samples in NMR tubes were subsequently subjected to NMR spectroscopy. The ^{1}H NMR spectra were recorded at 600 MHz on a Bruker AVANCE spectrometer (Bruker BioSpin GmbH, Germany) running Topspin 2.0 software. The metabolites were then quantified using the software Chenomx® NMR Suite 7.0™.

Statistical analysis

All statistical analysis and sample size are shown in each figure/table and in the corresponding figure/table legends, as well as in the Source of Data document. Only samples from viable fetuses were analysed. No statistical analysis was used to pre-determine sample size and samples were assigned code numbers and, were possible, analysis was performed in a blinded fashion. Statistical calculations were performed using the GraphPad Prism software (GraphPad v9, San Diego, CA), SAS/STAT 9.0 (Statistical System Institute Inc. Cary, NC, USA) and RStudio Version 1.4.1106 (RStudio Boston, MA) with R Version 4.0.3 (Vienna, Austria). Data reported as mean±SEM. Morphometric parameters of mother, number of viable/resorption per litter and western blot data were analysed by one-way ANOVA followed by Tukey post hoc test. Feto-placental weights, placental stereological measurements and placental Lz gene expression levels were analysed with a general linear mixed model, taking into account viable litter size as a covariate and taking each fetus as a repeated measure. In this statistical analysis, fetuses and placentas per litter are nested within litters[60]. Identification of outliers was performed with ROUT Method. For metabolomics, differences between individual metabolites between the three groups were tested with a Kruskal-Wallis test using the kruskal.test function with correction for multiple comparisons applied using the Benjamini & Hochberg false discovery rate method using the p.adjust function. Pairwise comparisons

between the three groups were carried out with a Dunn's test on individual metabolites significantly different after correction for multiple comparisons using the dunnTest function in the FSA package. The level of significance for all statistical tests used in this study was set at $P<0.05$. All figures in the manuscript show individual values (raw data). However, P values and mean±SEM within the graphs analysed by general linear mixed model were corrected for repeated measures. Graphs containing the individual dots and graphs with corrected mean±SEM were generated with Graphpad and merged with Adobe Illustrator.

Acknowledgments

JL-T currently holds a Sir Henry Wellcome Postdoctoral Fellowship (220456/Z/20/Z) and previously a Newton International Fellowship from the Royal Society (NF170988 / RG90199). LJH is supported by Wellcome Trust Investigator Awards (100974/C/13/Z and 220876/Z/20/Z); the Biotechnology and Biological Sciences Research Council (BBSRC), Institute Strategic Programme Gut Microbes and Health (BB/R012490/1), and its constituent projects BBS/E/F/000PR10353 and BBS/E/F/000PR10356. ANS-P is supported by a Lister Institute of Preventative Medicine Research Prize (RG93692). Authors would like to thank Dr Ruben Bermejo-Poza (Complutense University of Madrid) for statistical advice and the Ferguson-Smith laboratory (University of Cambridge) for providing the DLK1 antibody.

Data availability

The fetal liver RNA-Seq raw sequencing data are deposited at the National Center for Biotechnology Information (NCBI) under BioProject PRJNA748000. Relevant data are within the manuscript and its Supporting Information files. Scripts for differential gene expression

analysis can be accessed at GitHub, https://github.com/raymondkiu/Maternal-foetal-microbiota-paper/

References

1. Krajmalnik-Brown, R., Ilhan, Z.-E., Kang, D.-W. & DiBaise, J. K. Effects of Gut Microbes on Nutrient Absorption and Energy Regulation. *Nutr Clin Pract* **27**, 201–214 (2012).
2. McDonald, B. & McCoy, K. D. Maternal microbiota in pregnancy and early life. *Science* **365**, 984–985 (2019).
3. Agüero, M. G. de *et al.* The maternal microbiota drives early postnatal innate immune development. *Science* **351**, 1296–1302 (2016).
4. Koren, O. *et al.* Host remodeling of the gut microbiome and metabolic changes during pregnancy. *Cell* **150**, 470–480 (2012).
5. Nuriel-Ohayon, M. *et al.* Progesterone Increases Bifidobacterium Relative Abundance during Late Pregnancy. *Cell Rep* **27**, 730-736.e3 (2019).
6. Napso, T., Yong, H., Lopez-Tello, J. & Sferruzzi-Perri, A. N. The role of placental hormones in mediating maternal adaptations to support pregnancy and lactation. *Front. Physiol.* **9**, (2018).
7. Lamousé-Smith, E. S., Tzeng, A. & Starnbach, M. N. The intestinal flora is required to support antibody responses to systemic immunization in infant and germ free mice. *PLoS One* **6**, e27662 (2011).
8. Kennedy, E. A., King, K. Y. & Baldridge, M. T. Mouse Microbiota Models: Comparing Germ-Free Mice and Antibiotics Treatment as Tools for Modifying Gut Bacteria. *Frontiers in Physiology* **9**, 1534 (2018).
9. Lu, J. *et al.* Microbiota influence the development of the brain and behaviors in C57BL/6J mice. *PLoS One* **13**, e0201829 (2018).

10. Martin, A. M. *et al.* The gut microbiome regulates host glucose homeostasis via peripheral serotonin. *PNAS* **116**, 19802–19804 (2019).
11. Faas, M. M. *et al.* Microbiota Induced Changes in the Immune Response in Pregnant Mice. *Front Immunol* **10**, 2976 (2019).
12. Pokusaeva, K., Fitzgerald, G. F. & van Sinderen, D. Carbohydrate metabolism in Bifidobacteria. *Genes Nutr* **6**, 285–306 (2011).
13. Fanning, S. *et al.* Bifidobacterial surface-exopolysaccharide facilitates commensal-host interaction through immune modulation and pathogen protection. *PNAS* **109**, 2108–2113 (2012).
14. Kiu, R. *et al.* Bifidobacterium breve UCC2003 Induces a Distinct Global Transcriptomic Program in Neonatal Murine Intestinal Epithelial Cells. *iScience* **23**, 101336 (2020).
15. Liu, X. *et al.* Altered gut microbiome accompanying with placenta barrier dysfunction programs pregnant complications in mice caused by graphene oxide. *Ecotoxicology and Environmental Safety* **207**, 111143 (2021).
16. Single-cell RNA-Seq analysis reveals dynamic trajectories during mouse liver development - PubMed. https://pubmed.ncbi.nlm.nih.gov/29202695/.
17. Coan, P. M., Ferguson-Smith, A. C. & Burton, G. J. Developmental dynamics of the definitive mouse placenta assessed by stereology. *Biol Reprod* **70**, 1806–1813 (2004).
18. Dalby, M. J. & Hall, L. J. Recent advances in understanding the neonatal microbiome. *F1000Res* **9**, F1000 Faculty Rev-422 (2020).
19. Hughes, K. R. *et al.* Bifidobacterium breve reduces apoptotic epithelial cell shedding in an exopolysaccharide and MyD88-dependent manner. *Open Biol* **7**, 160155 (2017).
20. Miao, T. *et al.* Decrease in abundance of bacteria of the genus Bifidobacterium in gut microbiota may be related to pre-eclampsia progression in women from East China. *Food & Nutrition Research* (2021) doi:10.29219/fnr.v65.5781.

21. Fukuda, S. *et al.* Bifidobacteria can protect from enteropathogenic infection through production of acetate. *Nature* **469**, 543–547 (2011).
22. González Hernández, M. A., Canfora, E. E., Jocken, J. W. E. & Blaak, E. E. The Short-Chain Fatty Acid Acetate in Body Weight Control and Insulin Sensitivity. *Nutrients* **11**, 1943 (2019).
23. Priyadarshini, M. *et al.* Maternal short-chain fatty acids are associated with metabolic parameters in mothers and newborns. *Transl Res* **164**, 153–157 (2014).
24. Thorburn, A. N. *et al.* Evidence that asthma is a developmental origin disease influenced by maternal diet and bacterial metabolites. *Nat Commun* **6**, 7320 (2015).
25. Kim, C. H. Control of lymphocyte functions by gut microbiota-derived short-chain fatty acids. *Cell Mol Immunol* **18**, 1161–1171 (2021).
26. Kikuchi, K., Ben Othman, M. & Sakamoto, K. Sterilized bifidobacteria suppressed fat accumulation and blood glucose level. *Biochem Biophys Res Commun* **501**, 1041–1047 (2018).
27. Wu, H. *et al.* Metformin alters the gut microbiome of individuals with treatment-naive type 2 diabetes, contributing to the therapeutic effects of the drug. *Nat Med* **23**, 850–858 (2017).
28. Solito, A. *et al.* Supplementation with Bifidobacterium breve BR03 and B632 strains improved insulin sensitivity in children and adolescents with obesity in a cross-over, randomized double-blind placebo-controlled trial. *Clinical Nutrition* **40**, 4585–4594 (2021).
29. Aoki, R. *et al.* A proliferative probiotic Bifidobacterium strain in the gut ameliorates progression of metabolic disorders via microbiota modulation and acetate elevation. *Sci Rep* **7**, 43522 (2017).
30. López-Tello, J. *et al.* Fetal and trophoblast PI3K p110α have distinct roles in regulating resource supply to the growing fetus in mice. *Elife* **8**, (2019).
31. Frost, J. M. & Moore, G. E. The Importance of Imprinting in the Human Placenta. *PLOS Genetics* **6**, e1001015 (2010).
32. Sferruzzi-Perri, A. N., Sandovici, I., Constancia, M. & Fowden, A. L. Placental phenotype and the insulin-like growth factors: resource allocation to fetal growth. *J Physiol* **595**, 5057–5093 (2017).

33. Sferruzzi-Perri, A. N. *et al.* Placental-specific Igf2 deficiency alters developmental adaptations to undernutrition in mice. *Endocrinology* **152**, 3202–3212 (2011).

34. Sandovici, I. *et al. The Imprinted Igf2-Igf2r Axis is Critical for Matching Placental Microvasculature Expansion to Fetal Growth*. 520536 https://www.biorxiv.org/content/10.1101/520536v3 (2021) doi:10.1101/520536.

35. Yevtodiyenko, A. & Schmidt, J. V. Dlk1 expression marks developing endothelium and sites of branching morphogenesis in the mouse embryo and placenta. *Developmental Dynamics* **235**, 1115–1123 (2006).

36. Huang, C.-C. *et al.* Soluble delta-like 1 homolog (DLK1) stimulates angiogenesis through Notch1/Akt/eNOS signaling in endothelial cells. *Angiogenesis* **21**, 299–312 (2018).

37. Forbes, K., Westwood, M., Baker, P. N. & Aplin, J. D. Insulin-like growth factor I and II regulate the life cycle of trophoblast in the developing human placenta. *American Journal of Physiology-Cell Physiology* **294**, C1313–C1322 (2008).

38. Cuenda, A. & Rousseau, S. p38 MAP-Kinases pathway regulation, function and role in human diseases. *Biochimica et Biophysica Acta (BBA) - Molecular Cell Research* **1773**, 1358–1375 (2007).

39. Mudgett, J. S. *et al.* Essential role for p38α mitogen-activated protein kinase in placental angiogenesis. *PNAS* **97**, 10454–10459 (2000).

40. Sferruzzi-Perri, A. N., Higgins, J. S., Vaughan, O. R., Murray, A. J. & Fowden, A. L. Placental mitochondria adapt developmentally and in response to hypoxia to support fetal growth. *Proc. Natl. Acad. Sci. U.S.A.* **116**, 1621–1626 (2019).

41. Fan, Z., Han, Y., Ye, Y., Liu, C. & Cai, H. l-carnitine preserves cardiac function by activating p38 MAPK/Nrf2 signalling in hearts exposed to irradiation. *European Journal of Pharmacology* **804**, 7–12 (2017).

42. Ruiz, L., Delgado, S., Ruas-Madiedo, P., Sánchez, B. & Margolles, A. Bifidobacteria and Their Molecular Communication with the Immune System. *Front Microbiol* **8**, 2345 (2017).
43. Amabebe, E. & Anumba, D. O. C. Female Gut and Genital Tract Microbiota-Induced Crosstalk and Differential Effects of Short-Chain Fatty Acids on Immune Sequelae. *Frontiers in Immunology* **11**, 2184 (2020).
44. Mazé, A., O'Connell-Motherway, M., Fitzgerald, G. F., Deutscher, J. & Sinderen, D. van. Identification and Characterization of a Fructose Phosphotransferase System in Bifidobacterium breve UCC2003. *Applied and Environmental Microbiology* **73**, 545 (2007).
45. Cronin, M. *et al.* High Resolution In Vivo Bioluminescent Imaging for the Study of Bacterial Tumour Targeting. *PLOS ONE* **7**, e30940 (2012).
46. Musial, B. *et al.* Proximity to Delivery Alters Insulin Sensitivity and Glucose Metabolism in Pregnant Mice. *Diabetes* **65**, 851–860 (2016).
47. De Clercq, K., Lopez-Tello, J., Vriens, J. & Sferruzzi-Perri, A. N. Double-label immunohistochemistry to assess labyrinth structure of the mouse placenta with stereology. *Placenta* **94**, 44–47 (2020).
48. Salazar-Petres, E., Carvalho, D. P., Lopez-Tello, J. & Sferruzzi-Perri, A. N. *Placental mitochondrial function, nutrient transporters, metabolic signalling and steroid metabolism relate to fetal size and sex in mice*. 2021.07.22.453249 https://www.biorxiv.org/content/10.1101/2021.07.22.453249v1 (2021) doi:10.1101/2021.07.22.453249.
49. Romero-Calvo, I. *et al.* Reversible Ponceau staining as a loading control alternative to actin in Western blots. *Anal Biochem* **401**, 318–320 (2010).
50. Livak, K. J. & Schmittgen, T. D. Analysis of relative gene expression data using real-time quantitative PCR and the 2(-Delta Delta C(T)) Method. *Methods* **25**, 402–408 (2001).
51. Chen, S., Zhou, Y., Chen, Y. & Gu, J. fastp: an ultra-fast all-in-one FASTQ preprocessor. *Bioinformatics* **34**, i884–i890 (2018).

52. Kopylova, E., Noé, L. & Touzet, H. SortMeRNA: fast and accurate filtering of ribosomal RNAs in metatranscriptomic data. *Bioinformatics* **28**, 3211–3217 (2012).
53. Bray, N. L., Pimentel, H., Melsted, P. & Pachter, L. Near-optimal probabilistic RNA-seq quantification. *Nat Biotechnol* **34**, 525–527 (2016).
54. Zerbino, D. R. *et al.* Ensembl 2018. *Nucleic Acids Res* **46**, D754–D761 (2018).
55. Pimentel, H., Bray, N. L., Puente, S., Melsted, P. & Pachter, L. Differential analysis of RNA-seq incorporating quantification uncertainty. *Nat Methods* **14**, 687–690 (2017).
56. Kinsella, R. J. *et al.* Ensembl BioMarts: a hub for data retrieval across taxonomic space. *Database (Oxford)* **2011**, bar030 (2011).
57. Raudvere, U. *et al.* g:Profiler: a web server for functional enrichment analysis and conversions of gene lists (2019 update). *Nucleic Acids Res* **47**, W191–W198 (2019).
58. Le Gall, G. Sample collection and preparation of biofluids and extracts for NMR spectroscopy. *Methods Mol Biol* **1277**, 15–28 (2015).
59. Wu, J., An, Y., Yao, J., Wang, Y. & Tang, H. An optimised sample preparation method for NMR-based faecal metabonomic analysis. *Analyst* **135**, 1023–1030 (2010).
60. Lazic, S. E. & Essioux, L. Improving basic and translational science by accounting for litter-to-litter variation in animal models. *BMC Neuroscience* **14**, 37 (2013).

Figure 1. Effects of maternal gut microbiome and *B. breve* supplementation during pregnancy on fetal viability, growth and hepatic transcriptome. (A) Experimental design, **(B)** Number of viable fetuses per litter and (One-way ANOVA with Tukey's multiple comparison), **(C)** Number of resorptions per litter (left) and number of dams with presence of resorptions within the litter (right) (One-way ANOVA with Tukey's multiple comparison), **(D)** Fetal weight, **(E)** Fetal blood glucose concentrations, **(F)** Fetal organ weights. All data shown in

D to F were obtained on GD16.5 from: SPF (6 dams), GF (5 dams), BIF (6 dams). Dots represent raw data (individual values). However, the statistical analysis and the mean±SEM reported in the graphs were obtained with a general linear mixed model taking into account viable litter size as a covariate and taking each fetus as a repeated measure followed by Tukey multiple comparisons test (further explanations can be found in the Materials and Methods-statistical analysis section). Identification of outliers was performed with ROUT Method. **(G-J)** RNA-Seq analysis of fetal liver samples obtained at GD18.5, **(G)** PCA plot and **(H)** volcano plots showing up and down-regulated DEGs in BIF group (compared to GF group), **(I)** Heat map of the 20 most up and down-regulated DEGs (BIF group), **(J)** Functional profiling (g:Profiler) on 602 DEGs. Key enriched GO terms and REACTOME pathways are shown in the figure (significant threshold: $P_{adj}<0.001$). RNA-seq was performed on fetal livers obtained at GD18.5 from a total of 3 GF and 4 BIF pregnant dams/litters. RNA-Seq data analysis is described in the material and methods section. ($P<0.05$; mean±SEM).

Figure 2. Effects of maternal gut microbiome and *B. breve* supplementation during pregnancy on placental structure and placental gene expression on day 16.5 of gestation. (A) Placenta weight, **(B)** Placental efficiency determined by dividing fetal by placental mass, **(C)** Placental regional analysis, **(D)** Representative staining of placental glycogen with PAS and glycogen abundance, **(E)** Representative image of lectin and cytokeratin staining for labyrinth zone structural quantification, **(F-I)** Stereological parameters determined in placental labyrinth zone, **(J)** Representative image of TUNEL staining for apoptosis quantification in labyrinth zone, **(K)** Gene expression levels in micro-dissected

labyrinth zones, **(L)** Immunoblots and protein quantification by Western blot in micro-dissected labyrinth zones, **(M-P)** Gene expression levels in micro-dissected labyrinth zones. All data were analyzed by general linear mixed model, taking into account litter size as a covariate and taking each fetus as a repeated measure followed by Tukey multiple comparisons test. ROUT test was used for identification of outlier values. Dots represent raw data (individual values). However, the statistical analysis and the mean±SEM reported within the graphs were obtained with the general linear mixed model (further explanations can be found in the Materials and Methods statistical analysis section). Placental weight-efficiency was obtained from: SPF (6 dams), GF (5 dams), BIF (6 dams). Laboratorial analysis was performed with: SPF (6 dams), GF (5 dams) and BIF (6 dams). Only placentas collected on day 16.5 of gestation were analysed.

Figure 3. Metabolomic profiling of placental labyrinth zone and fetal liver on day 16.5 of gestation. Data were analysed by Kruskal-Wallis test followed by multiple comparisons using the Benjamini & Hochberg false discovery rate method and Dunn's test. ROUT test was used for identification of outlier values. Different superscripts indicate significant differences between groups (a *versus* b, $P<0.05$). Data presented as mean±SEM. Number of litters analysed per group: SPF (4 dams), GF (4-5 dams), BIF (5 dams). Only tissues collected at GD16.5 were analysed.

Figure 4. Summary illustration showing how the maternal gut bacteria and *B. breve* affects mother, placenta and fetus during gestation. Abbreviations: SPF (Specific-Pathogen-Free mouse); GF (Germ-Free mouse); BIF (Germ-Free mouse treated with *B. breve* UCC2003).

Supplementary Figure 1. Colonization levels of *B. breve* determined in maternal faecal samples on gestational day (GD), 12 and 14. Analysis performed by two-ways ANOVA (****P<0.0001). Data displayed as mean ± SEM. Number of dams for GF and BIF groups are 5 and 6, respectively. Assessment was performed only on dams sacrificed at GD16.5.

Supplementary Figure 2. Resorption rate was assessed only on day 16.5 of gestation and was defined as the number of resorptions divided by the sum of resorptions and viable fetuses within the litter. Data displayed as mean ± SEM and analysed by One-way ANOVA with Tukey's multiple comparison. Number of dams at day 16.5 of gestation: SPF (6), GF (5), BIF (6).

Table 1. Effects of maternal gut microbiome and *B. breve* administration during pregnancy on maternal body composition, circulating metabolites and hormones in maternal serum, and metabolites in caecum on day 16.5 of gestation. Body composition and metabolites/hormones in serum were analyzed by one-way ANOVA followed by Tukey multiple comparisons test. Metabolites in maternal caecum were analysed by Kruskal-Wallis test followed by multiple comparisons using the Benjamini & Hochberg false discovery rate method and Dunn's test. ROUT test was used for identification of outlier values. The level of significance was set at $P<0.05$. NS: not significant. Data presented as mean±SEM. The number of dams used for each group is annotated on the table and only data from dams at day 16.5 of gestation were used.

Supplementary Table 1. List of metabolites analysed in maternal caecum, placental labyrinth zone and fetal liver on day 16.5 of gestation.

Supplementary Table 2. List of differentially expressed genes and pathways detected in the liver RNA-Seq on day 18.5 of gestation.

Supplementary Table 3. List of primers used for placental labyrinth zone qPCR

Table 1. Body composition and circulating metabolites-hormones						
	SPF (n=6)	GF (n=5)	BIF (n=6)	SPF vs GF	SPF vs BIF	GF vs BIF
Hysterectomy weight (g)	26.01±0.91	27.87±0.78	27.17±0.80	NS	NS	NS
Digestive Tract (g)	2.76±0.03	6.83±0.32	7.25±0.63	<0.0001	<0.0001	NS
Caecum (g)	0.66±0.03	3.47±0.25	3.96±0.41	<0.0001	<0.0001	NS
Small intestine (g)	1.66±0.03	2.65±0.11	2.59±0.14	<0.0001	<0.0001	NS
Pancreas (mg)	315.40±30.12	183.40±24.74	190.60±38.71	0.041	0.044	NS
Gonadal fat (mg)	433.10±43.20	297.0±37.02	272.0±27.35	NS	0.016	NS
Liver (g)	2.09±0.10	1.79±0.05	1.55±0.08	NS	0.001	NS
Spleen (mg)	117.90±2.80	91.76±10.60	83.03±6.72	NS	0.0127	NS
Glucose (mmol/L)	8.08±0.78	8.38±1.18	8.88±0.74	NS	NS	NS
Insulin (µg/L)	0.12±0.004	0.19±0.05	0.20±0.06	NS	NS	NS
Leptin (pg/mL)	2465±177.1	2739±486	2425±303	NS	NS	NS
Cholesterol (mmol/L)	1.33±0.03	1.56±0.08	1.41±0.09	NS	NS	NS
Triglycerides (mmol/L)	1.54±0.08	1.79±0.14	1.50±0.11	NS	NS	NS
Free Fatty Acids (µmol/L)	890.6±101.3	1440±362	1092±114.5	NS	NS	NS
Maternal caecum metabolites						
	SPF (n=3)	GF (n=4)	BIF (n=5)	SPF vs GF	SPF vs BIF	GF vs BIF
Butyrate (mmol/Kg)	12.47±7.97	0.00±0.00	0.00±0.00	0.006	0.008	NS
Citrulline (mmol/Kg)	0.30±0.06	0.00±0.00	0.00±0.00	0.006	0.008	NS
Fucose (mmol/Kg)	0.08±0.01	0.00±0.00	0.00±0.00	0.006	0.008	NS
Isobutyrate (mmol/Kg)	0.41±0.24	0.00±0.00	0.00±0.00	0.006	0.008	NS
Isovalerate (mmol/Kg)	0.09±0.01	0.00±0.00	0.00±0.00	0.006	0.008	NS
Malonate (mmol/Kg)	0.09±0.02	0.00±0.00	0.00±0.00	0.006	0.008	NS
Methylamine (mmol/Kg)	0.05±0.02	0.00±0.00	0.00±0.00	0.006	0.008	NS
Propionate (mmol/Kg)	4.48±1.99	0.00±0.00	0.00±0.00	0.006	0.008	NS
Trimethylamine (mmol/Kg)	0.06±0.007	0.00±0.00	0.00±0.00	0.006	0.008	NS
Valerate (mmol/Kg)	0.57±0.27	0.00±0.00	0.00±0.00	0.006	0.008	NS
2.methylbutyrate (mmol/Kg)	0.05±0.01	0.00±0.00	0.00±0.00	0.006	0.008	NS
5.Aminopentanoate (mmol/Kg)	0.33±0.14	0.00±0.00	0.00±0.00	0.006	0.008	NS
Acetate (mmol/Kg)	35.49±20.66	0.55±0.06	3.22±1.39	0.006	0.129	0.094

Supplementary Table 3	*Forward*	*Reverse*
Hprt	*CAGGCCAGACTTTGTTGGAT*	*TTGCGCTCATCTTAGGCTTT*
Ubc	*GGAGTCGCCCGAGGTCA*	*AAAGATCTGCATCGTCTCTCTCAC*
Vegf	*GAAGCTACTGCCGTCCGATT*	*CTTCATCGTTACAGCAGCC*
Akt	*GCCGCCTGATCAAGTTCTCC*	*TTCAGATGATCCATGCGGGG*
Mapk1	*TGCTTTCTCTCCCGCACAAA*	*GGCCAGAGCCTGTTCAACTT*
Mapk14	*AGCTGTCGAGACCGTTTCAG*	*GATGGGTCACCAGGTACACG*
Dlk1	*GAAAGGACTGCCAGCACAAG*	*CACAGAAGTTGCCTGAGAAGC*
Igf2P0	*GAGGAAGCTCTGCTGTTTGG*	*CAAAGAGATGAGAAGCACCAAC*
Hsd11b1	*GAGGAAGGTCTCCAGAAGGTA*	*ATGTCCAGTCCGCCCAT*
Hsd11b2	*GGCTGGATCGCGTTGTC*	*CGTGAAGCCCATGGCAT*
Slc38a1	*CGGCGCCTTTCCCTTTATTTC*	*CCGTTAACTCGAGGCCACTT*
Slc38a2	*TTCTGATTGTGGTGATTTGCAAGAA*	*CAGGATGGGCACAGCATACA*
Slc38a4	*AAGGTAGAGGCGGGAAAGGG*	*AGGAACTTCTGACTTTCGGCA*
Slc2a1	*GCTTATGGGCTTCTCCAAACT*	*GGTGACACCTCTCCCACATAC*
Slc2a3	*GA TCGGCTCTTTCCAGTTTG*	*CAA TCA TGCCACCAACAGAG*
Cd36	*ATGGGCTGTGATCGGAACTG*	*GTCTTCCCAATAAGCATGTCTCC*
Fatp1	*GGCTCCTGGAGCAGGAACA*	*ACGGAAGTCCCAGAAACCAA*
Fatp3	*GAGAACTTGCCACCGTATGC*	*GGCCCCTATATCTTGGTCCA*
Fatp4	*GATTCTCCCTGTTGCTCCTGT*	*CCATTGAAGCAAACAGCAGG*
Fatp6	*AACCAAGTGGTGACATCTCTGC*	*TCCATAAAGTAAAGCGGGTCAG*

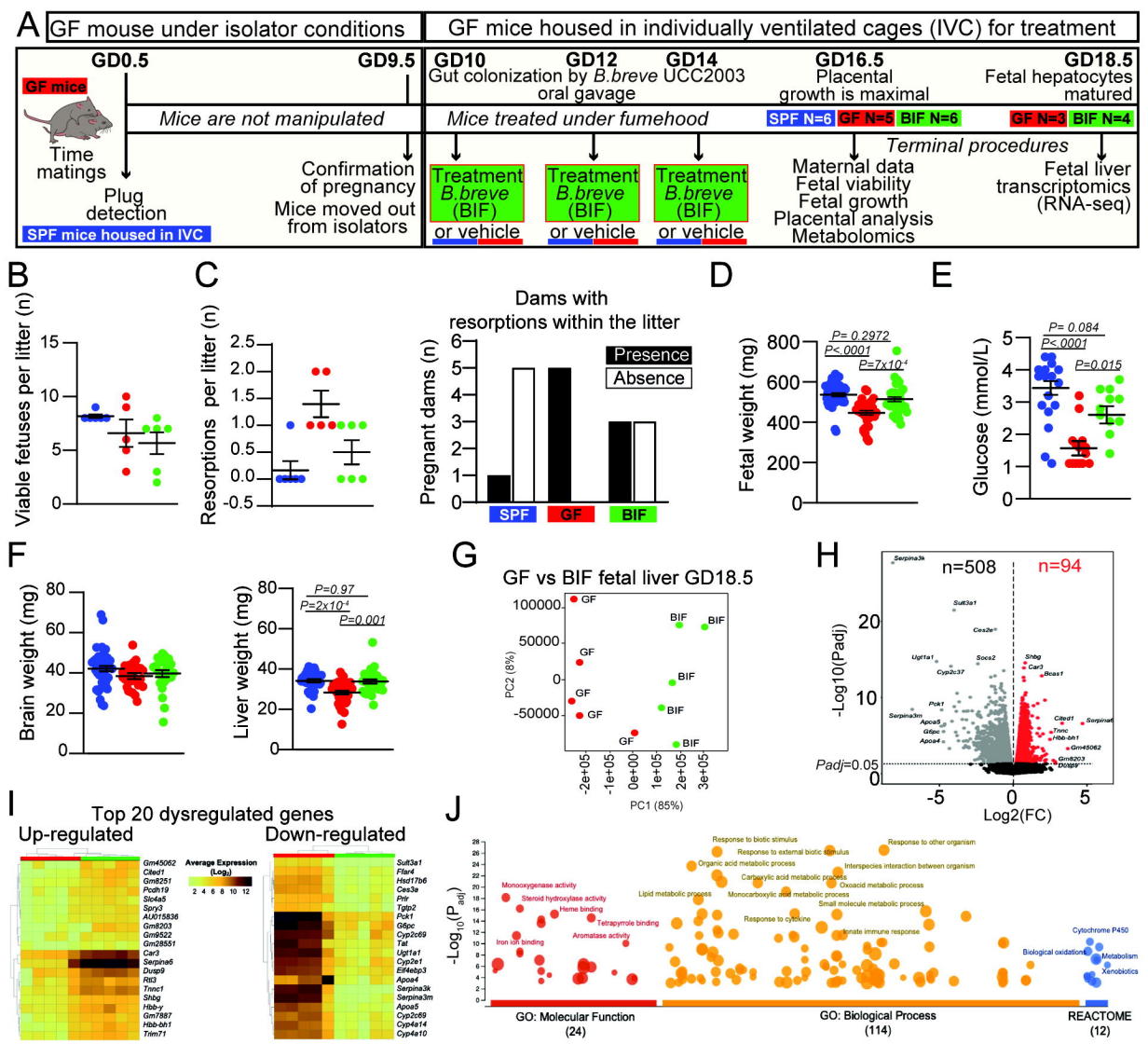
A
GF mouse under isolator conditions
GF mice housed in individually ventilated cages (IVC) for treatment
GD0.5
GD9.5
GF mice
Time matings
Plug detection
SPF mice housed in IVC
Mice are not manipulated
Confirmation of pregnancy
Mice moved out from isolators
GD10
GD12
GD14
GD16.5
GD18.5
Gut colonization by B.breve UCC2003 oral gavage
Placental growth is maximal
Fetal hepatocytes matured
Mice treated under fumehood
SPF N=6
GF N=5
BIF N=6
GF N=3
BIF N=4
Terminal procedures
Treatment B.breve (BIF) or vehicle
Maternal data
Fetal viability
Fetal growth
Placental analysis
Metabolomics
Fetal liver transcriptomics (RNA-seq)
B
Viable fetuses per litter (n)
C
Resorptions per litter (n)
Dams with resorptions within the litter
Pregnant dams (n)
Presence
Absence
SPF
GF
BIF
D
Fetal weight (mg)
P= 0.2972
P<.0001
P=7x10-4
E
Glucose (mmol/L)
P= 0.084
P<.0001
P=0.015
F
Brain weight (mg)
Liver weight (mg)
P=0.97
P=2x10-4
P=0.001
G
GF vs BIF fetal liver GD18.5
PC2 (8%)
PC1 (85%)
H
n=508
n=94
-Log10(Padj)
Padj=0.05
Log2(FC)
I
Top 20 dysregulated genes
Up-regulated
Down-regulated
Average Expression (Log2)
Gm45062
Cfad1
Gm8251
Pcdh19
Slc4a5
Spry3
AU015836
Gm8203
Gm9522
Gm28551
Car3
Serpina6
Dusp9
Rit3
Tnnc1
Shbg
Hbb-y
Gm7887
Hbb-bh1
Trim71
Sult3a1
Ftar4
Hsd17b6
Ces3a
Ptir
Tgfp2
Pck1
G6pc
Cyp2c69
Tat
Ugt1a1
Cyp2e1
Elf4ebp3
Apoa4
Serpina3k
Serpina3m
Apoa5
Cyp2c69
Cyp4a14
Cyp4a10
J
-Log10(Padj)
Response to biotic stimulus
Response to other organism
Response to external biotic stimulus
Organic acid metabolic process
Interspecies interaction between organism
Carboxylic acid metabolic process
Oxoacid metabolic process
Monocarboxylic acid metabolic process
Small molecule metabolic process
Monooxygenase activity
Steroid hydroxylase activity
Heme binding
Lipid metabolic process
Tetrapyrrole binding
Response to cytokine
Innate immune response
Aromatase activity
Iron ion binding
Cytochrome P450
Biological oxidation
Metabolism
Xenobiotics
GO: Molecular Function (24)
GO: Biological Process (114)
REACTOME (12)

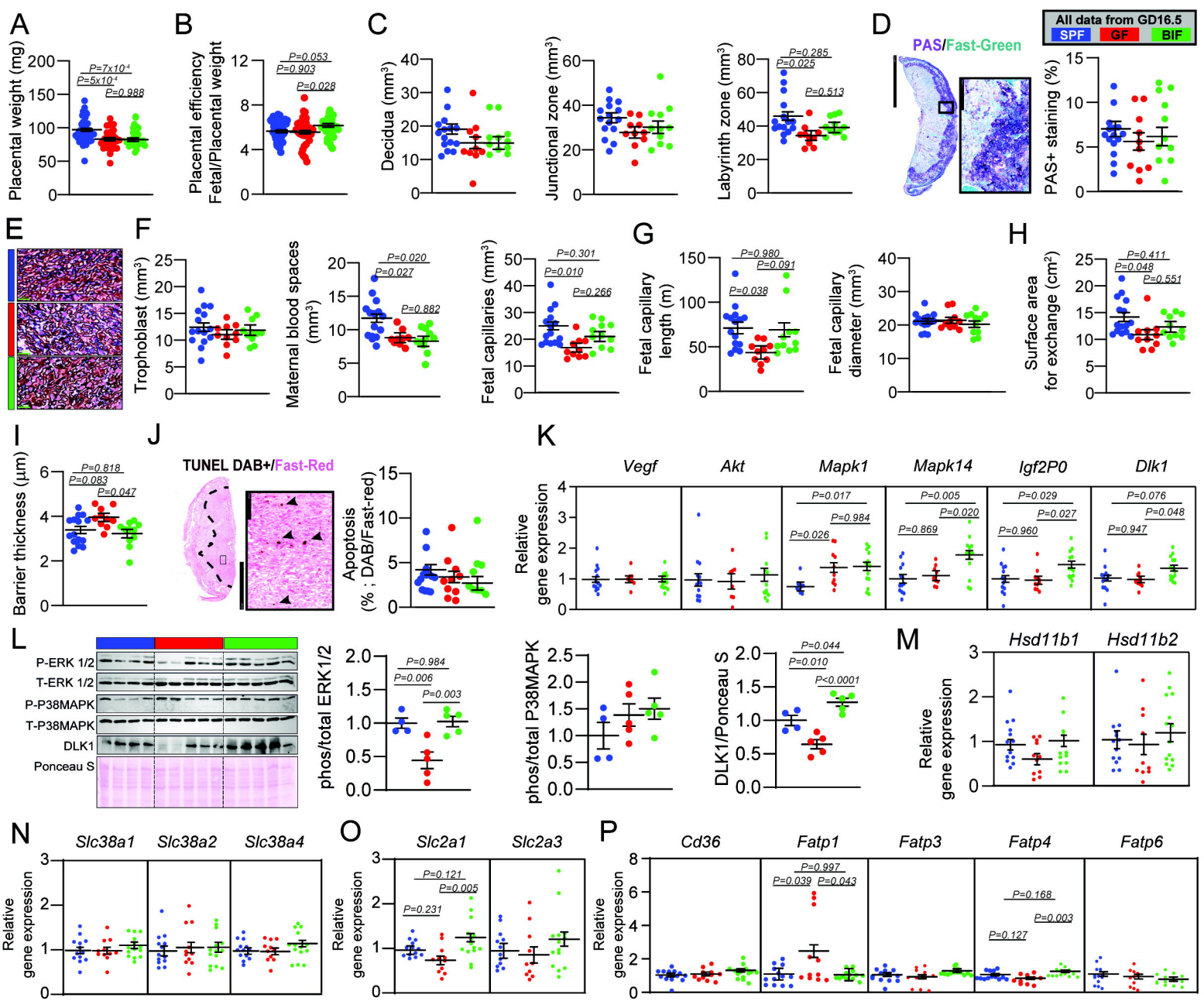
A
Placental weight (mg)
P=7x10-4
P=5x10-4
P=0.988
B
Placental efficiency Fetal/Placental weight
P=0.053
P=0.903
P=0.028
C
Decidua (mm3)
Junctional zone (mm3)
Labyrinth zone (mm3)
P=0.285
P=0.025
P=0.513
D
PAS/Fast-Green
All data from GD16.5
SPF
GF
BIF
PAS+ staining (%)
E
F
Trophoblast (mm3)
Maternal blood spaces (mm3)
P=0.020
P=0.027
P=0.882
Fetal capillaries (mm3)
P=0.301
P=0.010
P=0.266
G
Fetal capillary length (m)
P=0.980
P=0.091
P=0.038
Fetal capillary diameter (mm3)
H
Surface area for exchange (cm2)
P=0.411
P=0.048
P=0.551
I
Barrier thickness (µm)
P=0.818
P=0.083
P=0.047
J
TUNEL DAB+/Fast-Red
Apoptosis (% ; DAB/Fast-red)
K
Vegf
Akt
Mapk1
Mapk14
Igf2P0
Dlk1
Relative gene expression
P=0.017
P=0.984
P=0.026
P=0.005
P=0.020
P=0.869
P=0.029
P=0.027
P=0.960
P=0.076
P=0.048
P=0.947
L
P-ERK 1/2
T-ERK 1/2
P-P38MAPK
T-P38MAPK
DLK1
Ponceau S
phos/total ERK1/2
P=0.984
P=0.006
P=0.003
phos/total P38MAPK
DLK1/Ponceau S
P=0.044
P=0.010
P<0.0001
M
Hsd11b1
Hsd11b2
Relative gene expression
N
Slc38a1
Slc38a2
Slc38a4
Relative gene expression
O
Slc2a1
Slc2a3
Relative gene expression
P=0.121
P=0.005
P=0.231
P
Cd36
Fatp1
Fatp3
Fatp4
Fatp6
Relative gene expression
P=0.997
P=0.039
P=0.043
P=0.168
P=0.003
P=0.127

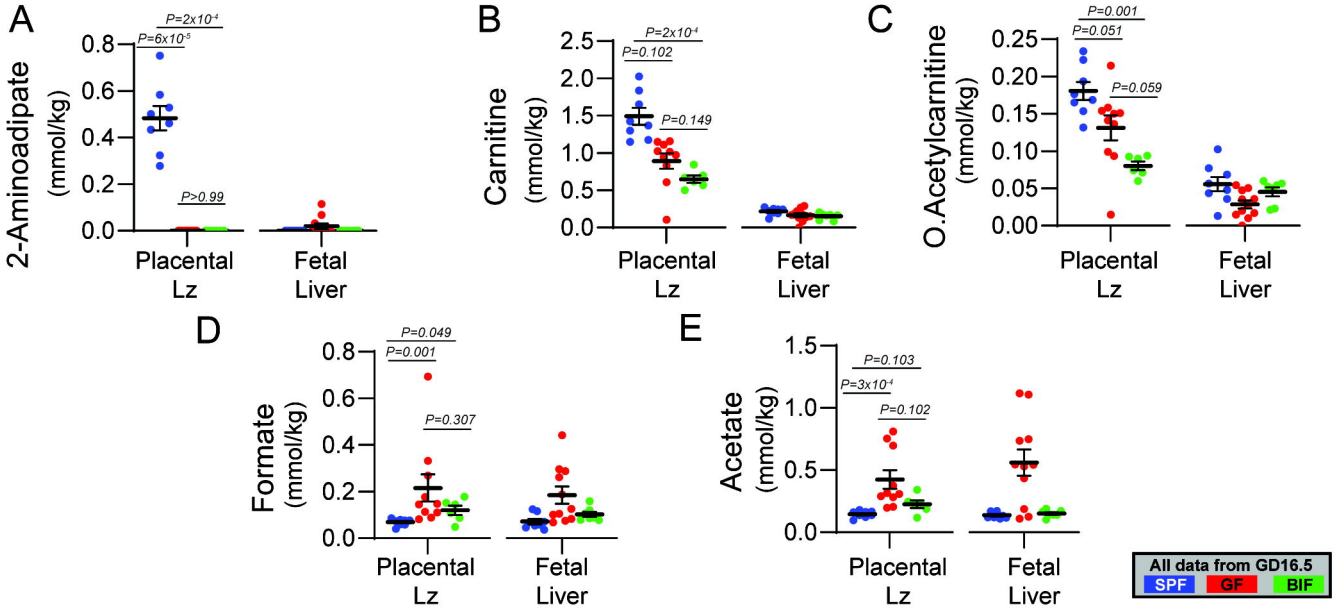
A
2-Aminoadipate
(mmol/kg)
P=2x10-4
P=6x10-5
P>0.99
Placental Lz
Fetal Liver
B
Carnitine
(mmol/kg)
P=2x10-4
P=0.102
P=0.149
C
O.Acetylcarnitine
(mmol/kg)
P=0.001
P=0.051
P=0.059
D
Formate
(mmol/kg)
P=0.049
P=0.001
P=0.307
E
Acetate
(mmol/kg)
P=0.103
P=3x10-4
P=0.102
All data from GD16.5
SPF
GF
BIF

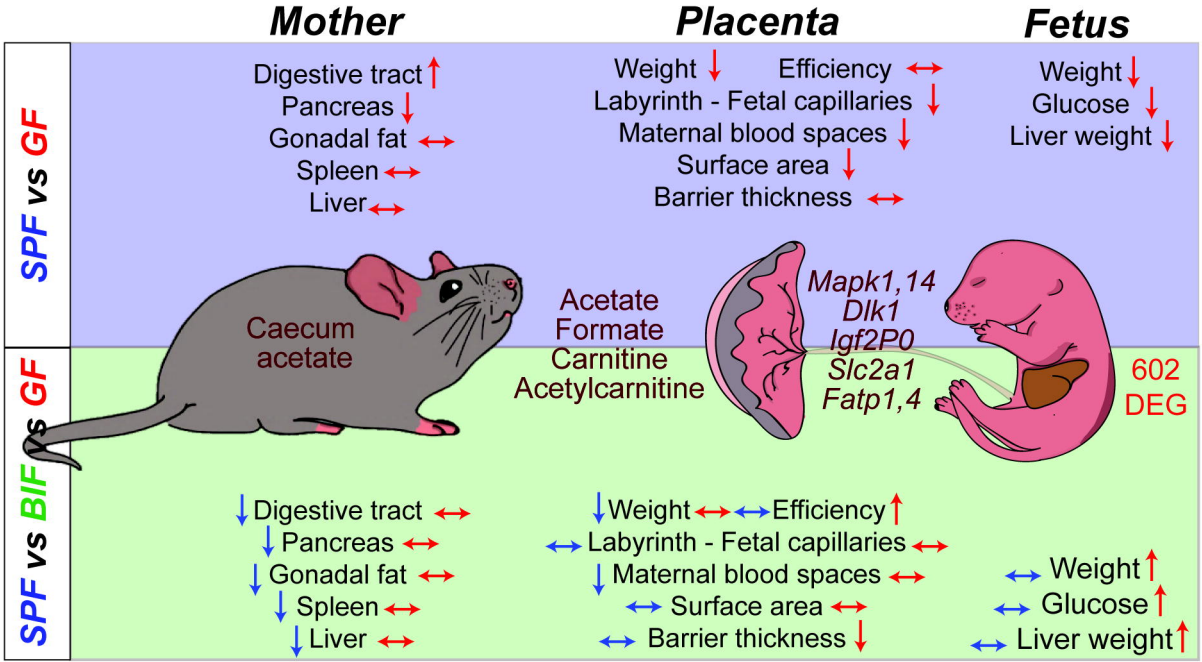

Additional caecum metabolites: Butyrate, Citrulline, Fucose, Isobutyrate, Isovalerate, Malonate, Methylamine, Propionate, Trimethylamine, Valerate, 2.methylbutyrate, 5.Aminopentanoate

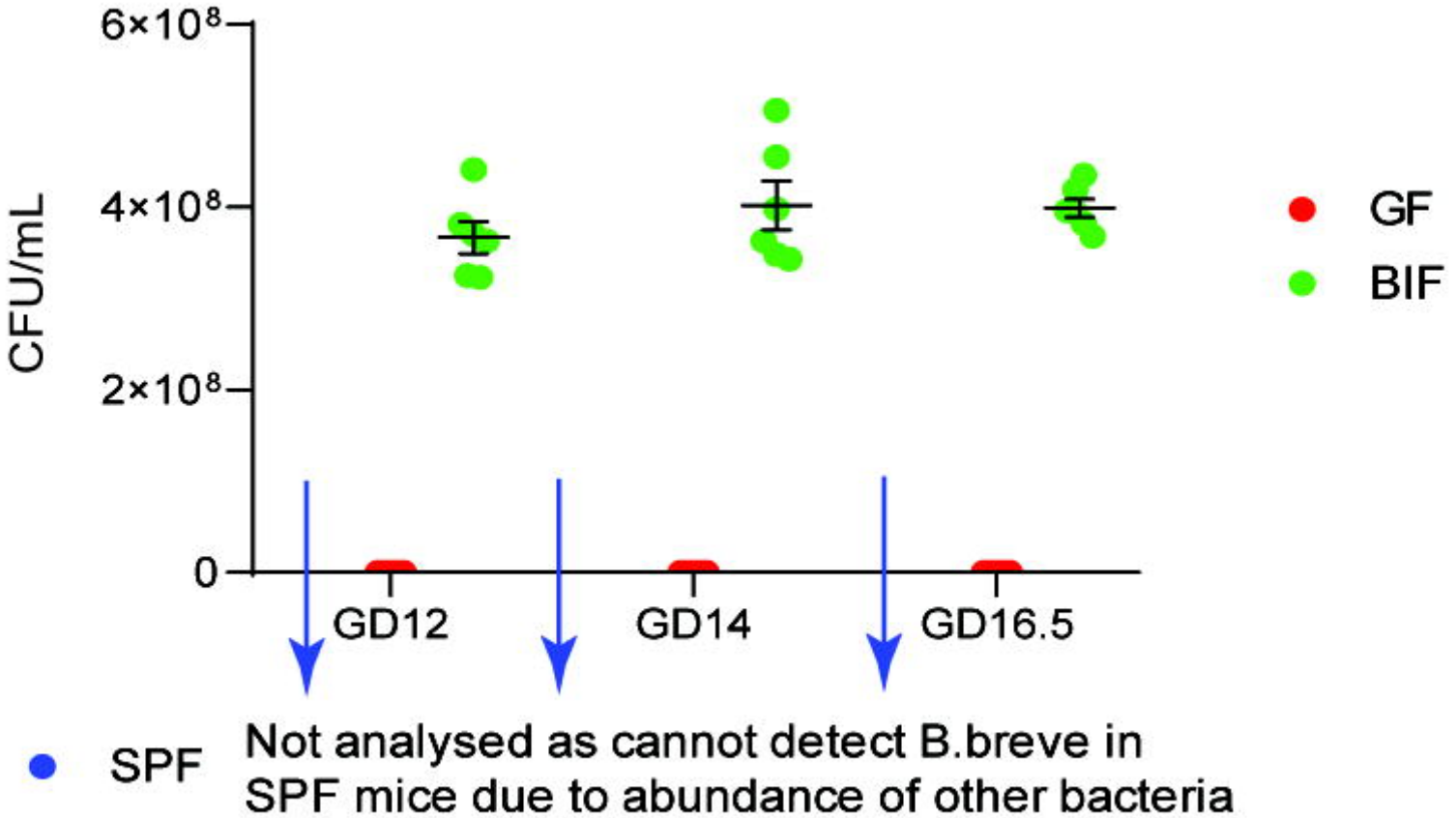
6×10⁸
4×10⁸
2×10⁸
0
CFU/mL
GD12
GD14
GD16.5
GF
BIF
SPF
Not analysed as cannot detect B.breve in SPF mice due to abundance of other bacteria

A

Group	TOTAL LITTER*	Viable	Resorption	Resportion rate (%)
SPF	8	8	0	0.00
SPF	8	8	0	0.00
SPF	9	8	1	11.11
SPF	9	9	0	0.00
SPF	8	8	0	0.00
SPF	8	8	0	0.00
GF	4	3	1	25.00
GF	12	10	2	16.67
GF	10	9	1	10.00
GF	8	6	2	25.00
GF	6	5	1	16.67
BIF	8	7	1	12.50
BIF	8	8	0	0.00
BIF	2	2	0	0.00
BIF	3	3	0	0.00
BIF	8	7	1	12.50
BIF	8	7	1	12.50

*** total litter is defined as: viable+resorptions**
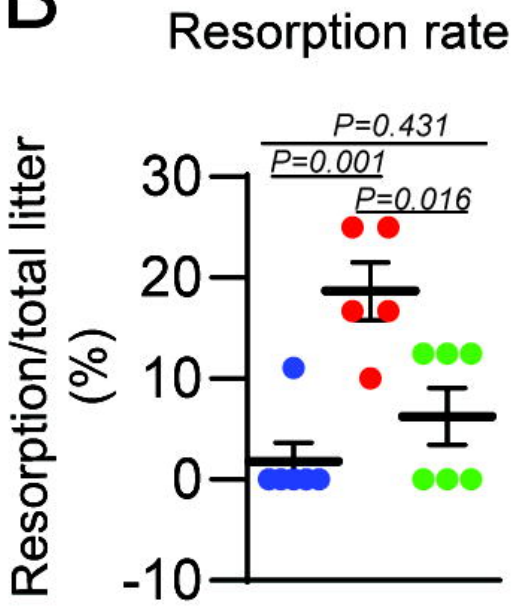
B